Sensors and Actuators B 227 (2016) 475–481

Contents lists available at ScienceDirect

Sensors and Actuators B: Chemical

journal homepage: www.elsevier.com/locate/snb

Applications for rapid formaldehyde nanoreactor with hierarchical and spherical structure

Ying Wang [a], Dingsheng Jiang [a], Wei Wei [b], Linghui Zhu [a], Jingran Zhou [a,*], Dongming Sun [a], Shengping Ruan [b,*]

[a] State Key Laboratory on Integrated Optoelectronics, Jilin University, Changchun 130012, PR China
[b] College of Electronic Science and Engineering, Jilin University, Changchun 130012, PR China

ARTICLE INFO

Article history:
Received 14 August 2015
Received in revised form
11 December 2015
Accepted 17 December 2015
Available online 24 December 2015

Keywords:
Mesoporous structure
Rapid response
Nanoreactor
Formaldehyde

ABSTRACT

Cu@SnO_2 spherical nanoreactor with hierarchical structure was prepared through a simple solvothermal method, the structure and morphology were characterized by X-ray diffraction (XRD) and scanning electron microscopy (SEM) showing the materials with extraordinary 3D nanoarchitectures. The gas sensing properties of the as-prepared pure SnO_2 and Cu-doped SnO_2 were tested toward various gases. The results showed that Cu-doped SnO_2 sensor displayed an excellent selectivity toward formaldehyde at the operating temperature 230 °C, which was much lower than most formaldehyde sensor in heater type among previous reports. The τrec and the τrec values of the Cu-doped SnO_2 to 1000 ppm formaldehyde were 2 s and 2 s, respectively, demonstrating extraordinary gas sensing properties, while those of the pure SnO_2 sensor were relatively long. The enhancement might be attributed to increased oxygen vacancy due to formation of active centers around doped elements and broad surface of unique mesoporous structure.

1. Introduction

Unique morphologies involving porous structure have frequently developed. Hierarchical structures composed by low dimensional blocks and porous oxide structures with well-aligned pore structures were studied by many reports [1]. Hierarchical nanostructures are the higher dimensional structures consisted of low dimensional structure, nanoscale blocks such as 0D nanoparticles, 1D nanofibers, and 2D nanosheets. In addition, hierarchical nanostructures show well-aligned porous structures with high surface area and less agglomerated configuration, while the non-agglomerated form of oxide nanoparticles is extremely difficult to accomplish. It should be known that beside higher dimensional morphology, hollow structure also attracts considerable attention because of their hollow interior architectures, which endow them not only with high specific areas and abundant inner voids, but also with controllable physical and chemical microenvironment. Compared with other techniques, solvothermal method possesses unique advantages, such as being simple but efficient, adaptable and less demanding for processing conditions. What's more, solvothermal processes may be used to control shape for fabrication of different dimensional nanomaterials [2]. Metal oxide materials made by these methods can exhibit unique application potential in microscopic physics and nano-devices [3].

As we all known that SnO_2 is one of the most important metal oxides, which has high temperature stability, with a direct bandgap of 3.6 eV, harsh environment tolerance and high surface reactivity. It has been widely used as gas sensing materials to detect gases such as C_2H_5OH, CO, NO_2, H_2S, due to its strong interaction with gas molecules and well controlled morphology [4]. Productive, low-cost and effective strategies for fabrication of nanomaterials with high specific surface area are urgently expected in potential applications of different applications.

In the past decades, amounts of analytical methods for the detection of VOCs have been reported, containing spectrophotometry [5], optical sensor detection [6] and ion chromatography [7] which are usually expensive requiring high energy-consumption and complex operation procedure, and unable to provide VOCs exposure information on a real-time basis. Thus, detection of gaseous formaldehyde (HCHO) is so difficult, leading to highly challenging to quantify and monitor. To maintain environmental safety, gas sensors are required for examining poisonous and hazardous gases, which have been widely applied in the fields of healthcare, safety, environmental monitoring and chemical process control since the introduction of chemical sensors [8–11]. Over the years, researchers have developed different sensors closely related to

* Corresponding authors. Fax: +86 431 85168242.
E-mail addresses: zhoujr@jlu.edu.cn (J. Zhou), ruansp@jlu.edu.cn (S. Ruan).

http://dx.doi.org/10.1016/j.snb.2015.12.063
0925-4005/

both species and morphologies. With the rapid development of nanoscience and technology, considerable efforts have been made to synthesis of new-type material.

In present work, Cu@SnO_2 microspheres formed by 2D nanosheets with mesoporous and hierarchical structure were successfully fabricated by using elaborately designed experimental scheme of one-step solvothermal method. Their super formaldehyde sensing properties and response mechanism were investigated via a convenient and lossless measurement technique which was reported for the first time. Highly efficient sensing performance against formaldehyde was observed, which is much better than published reports, making the fabricated material a good candidate sensing material for high performance formaldehyde sensors.

2. Experimental

2.1. Materials synthesis

All the used chemical reagents in this work were analytical grade and used as purchased without further purification: $SnCl_2{\cdot}2H_2O$, $Cu(NO_3)_2{\cdot}3H_2O$, NaOH, $Na_3C_6H_5O_7{\cdot}2H_2O$.

In a typical procedure, Cu@SnO_2 microspheres were synthesized by a typical solvothermal method. Firstly, certain volumes of ethanol (15 mL) were dissolved in deionized water (15 mL) to form a clear solution, then $SnCl_2{\cdot}2H_2O$ (0.9 g), NaOH(4 mmol), sodium citrate(1 mmol) and certain amount of $Cu(NO_3)_2{\cdot}3H_2O$ (the molar ratio of Cu to Sn is 0.062) were added into above solution under constant stirring. After stirred vigorously for 5 h, the solutions were transferred into 50 mL Teon-lined stainless steel autoclaves. The autoclaves were heated at 180 °C for 10 h, and then cooled down to room temperature naturally. The precipitates were separated by centrifugation, washed with distilled water and ethanol 5 times, and dried at 80 °C for 24 h. Finally, microspheres with hierarchical structure were obtained. We referred to these samples as S0 and S1, representing pure SnO_2 and the Cu@SnO_2, respectively.

2.2. Characterization

X-Ray diffraction (XRD) analysis was conducted on a Scintag XDS-2000 X-ray diffractometer with Cu Kα radiation (λ = 1.5418 Å) to analyze the structure of the prepared products. Scanning electron microscopy (SEM) images were performed on a SHIMADZU SSX-550 (Japan) instrument to observe the morphology of the prepared products. Transmission electron microscope (TEM) images were obtained on a JEM-ARM200F microscope to observe detailed microstructures and detect elements of the prepared products, respectively.

2.3. Fabrication and measurement of gas sensor

The as-prepared material was mixed with deionized water in a weight ratio of 4:1 and ground in a mortar for 3 h to form a paste. The paste was then coated on an Al_2O_3 ceramic tube to form a sensing film (a thickness of about 300 μm) on which a couple of parallel Au electrodes was previously printed. Pt lead wires attached to these Au electrodes were used as electrical contacts. After the ceramic tube was calcined at 300 °C for 2 h, a Ni–Cr heating wire was inserted into the ceramic tube as a heater for controlling the operating temperature. The structure of a sensor is shown in Fig. 1. The details of the sensor fabrication were similar to our previous works [12].

Gas sensing properties were measured by CGS-8 intelligent gas sensing analysis system (Beijing Elite Tech Co., Ltd., China) under laboratory condition (25 °C, 40 RH%). The response value (S) was defined as $S = (R_a - R_g)/R_a \times 100\%$, where R_a and R_g denoted the sensor's resistance in the air and presence of the target gases. The time taken by the sensor to achieve 90% of the total resistance change was defined as response time when the target gas was introduced to the sensor (target gas adsorption) or the recovery time when the chamber was full of air replacing target gas (target gas desorption) [13].

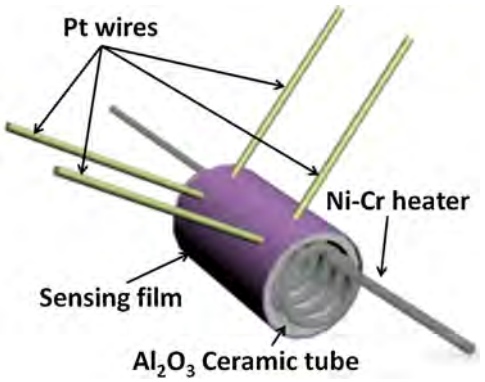

Fig. 1. Illustration of a gas sensor coated with sensing material.

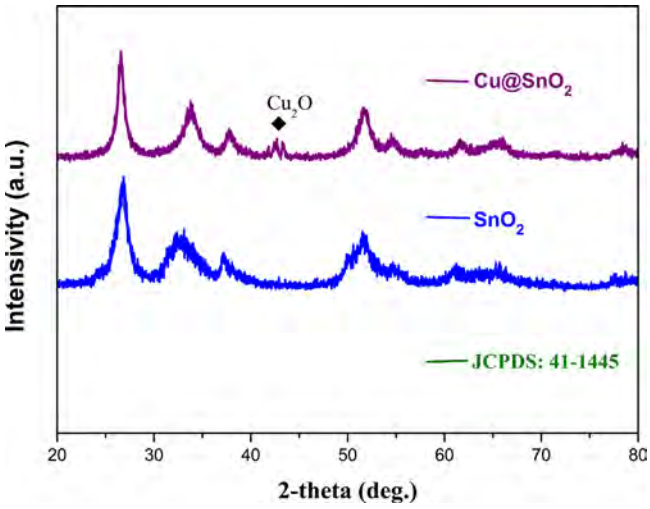

Fig. 2. XRD patterns of pure SnO_2 and Cu@SnO_2.

3. Results and discussion

3.1. Structural and morphological characteristics

The XRD patterns of S0 and S1 are shown in Fig. 2. It can be observed that all of the diffraction peaks of S0 and most peaks of S1 can be indexed to SnO_2, which were consistent with the Joint Committee on Powder Diffraction Standards card (JCPDS, 41-1445). The characteristic peak of Cu_2O (JCPDS, 35-1091) was also found, manifesting the place in lattice atom of Sn^{4+} was substituted by Cu^+. Therefore, the required products were successfully prepared.

To get further information about the unique architecture, SEM analysis was performed. The morphologies and nanostructures of the as-prepared S0 and S1 were characterized using FESEM (field emission scanning electron microscopy) as shown in Fig. 3. (a) and (b) displayed SEM images of S0; (c) and (d) displayed the SEM images of S1 in different magnifications.

Fig. 3(a) is the enlarged FESEM of a single sphere, showing that the sphere-like architectures consist of many nanosheets, estimated a diametral quotient in 1.8 μm and thickness in 25 nm.

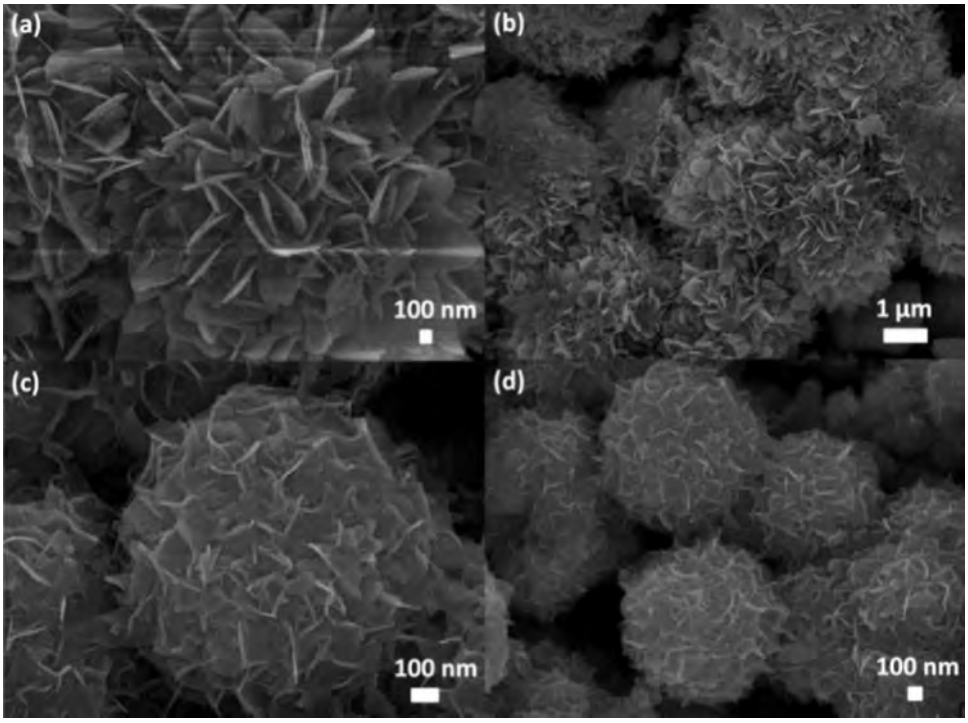

Fig. 3. High (a) and low (b) magnification SEM images of pure SnO_2 (S0); high (c) and low (d) magnification SEM images of Cu@ SnO_2 (S1).

No other morphologies could be detected in Fig. 3(b), and it is clear from the image that all the 3D structures were sphere-like architectures, with a diameter range of 2 ± 0.3 μm, which further confirming to result of Fig. 3(a). The high-magnification FESEM (Fig. 3(c)) shows the detailed morphological information of the sample S1, and it reveals diameter and thickness of the sphere nanostructure are about 1.5 μm and 15 nm. Fig. 3(d) is the as-prepared hierarchical architectures self-organized spheres of sample S1. It reveals all of spheres are of homogeneous dimensions, implied the overall size of each sphere ranges from 1.3 ± 0.2 μm horizontally and 15 ± 2 nm vertically, which is well accordance with estimations of Fig. 3(c), confirming the successful formation of Cu@SnO_2. Moreover, the diameter size and nanosheets thickness of S1 are obviously smaller than that of S0, which may result in the better gas sensing performances of S1 compared with S0.

3.2. Gas sensor performance

We all know that the gas response of a semiconductor sensor is usually dependent on sensor's operating temperature [13]. The optimum working temperature is determined by highest response of the sensor to test gas. As shown in Fig. 4, the responses of the sensors based on S0 and S1 to 100 ppm formaldehyde (HCHO) were tested to determine the optimum operating temperature. The preparation of 100 ppm HCHO sample gas was as followed: 0.307 μL of 37% formaldehyde solution was injected into 1 L gas bottle so as to evaporate into steam formaldehyde, other concentrations of sample gases were obtained by comparing the preparation of 100 ppm HCHO sample gas to a different volume of formaldehyde solution. It can be observed that the responses of the tested sensor varied with operating temperature. According to Fig. 4, 230 °C was suggested to be the optimum operating temperature for formaldehyde detection based on S0 and S1 sensors, because both sensors increased rapidly and showed the maximum response of 48.19 and 77.97 at the corresponding temperature and then followed by decrease with increasing operating temperature. It is apparently that the response of S1 sensor is higher than that of pure S0

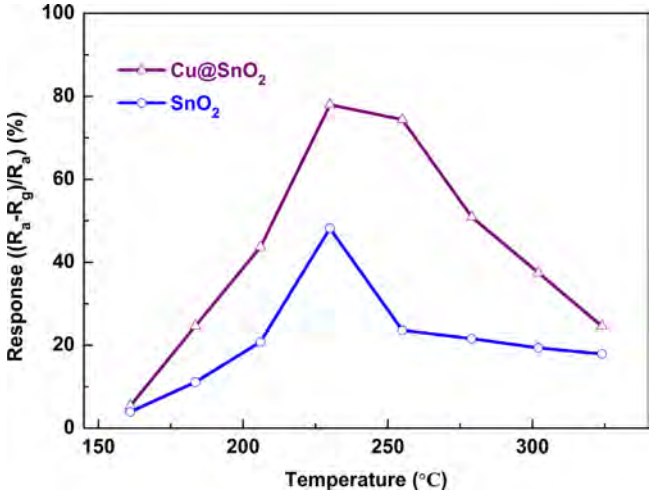

Fig. 4. Responses of sensors based on S0 and S1 to 100 ppm formaldehyde as a function of operating temperature.

sensor at same temperature and increased by nearly 162%, showing a better gas sensing property. Thus, the temperature 230 °C was correspondingly identified as the optimum operating temperature for both sensors and applied in all the investigations hereinafter. Furthermore, our gas sensor has a relatively low working temperature than those formaldehyde sensors based on Fe_2O_3–In_2O_3 nanotube (250 °C) [14], CuO nanocubes (300 °C) [15], and ZnO nanocones (275 °C) [16]. Operating temperature comparison of various sensors toward formaldehyde is shown in Table 1.

The reason why the sensor based on S1 shows the highest response to formaldehyde at 230 °C maybe as follows: The increase of operating temperature could facilitate the chemical reaction on the material surface, which will lead to the increase of response in lower temperature. Moreover, desorption of HCHO molecules process was accelerated with the rising of temperature, while adsorption HCHO molecules process was impeded. As the reaction

Table 1
Operating temperature comparison of various gas sensors toward formaldehyde.

Material	Preparation method	Concentration (ppm)	Operating temperature (°C)
SnO_2/In_2O_3 [17]	Electrospinning	10	375
In_2O_3 [18]	Chemical spray pytolysis	80	275
SnO_2 [19]	Topological transformation	100	330
$Fe_3O_4@Co_3O_4$ [2]	Hydrothermal	100	240
$Cu@SnO_2$ in this paper	Solvothermal	100	230

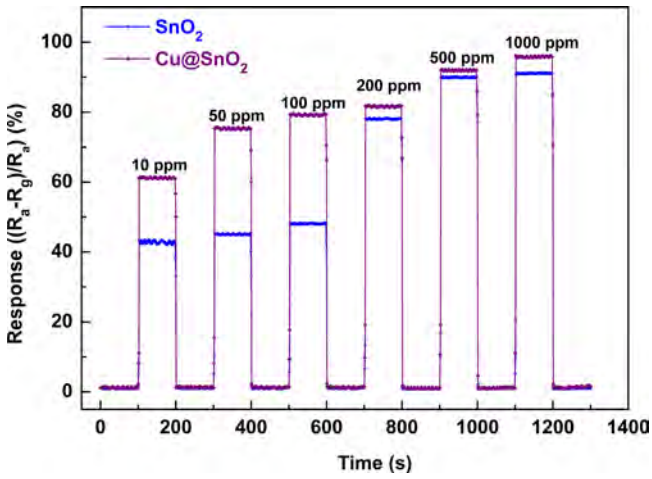

Fig. 5. Sensing transients of S0 and S1 sensors to 10–1000 ppm formaldehyde at 230 °C.

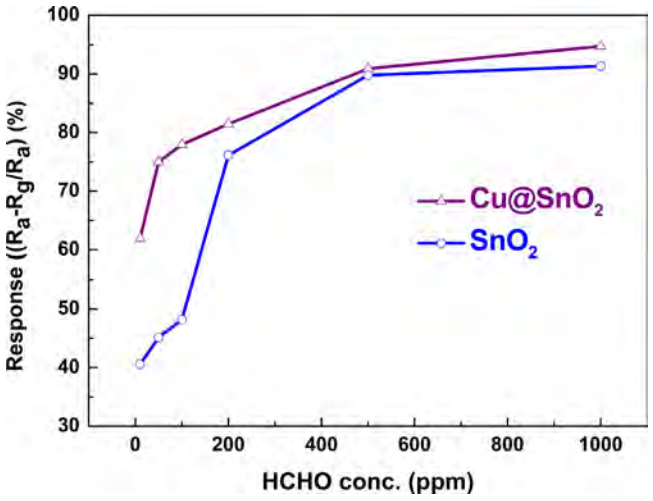

Fig. 6. Responses of sensors based on S0 and S1 at 230 °C versus formaldehyde.

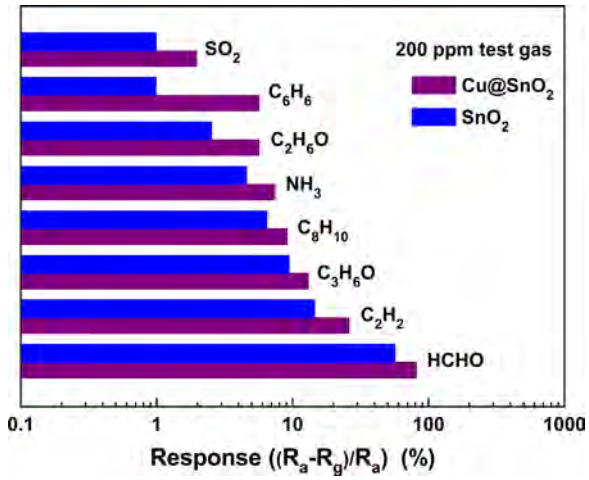

Fig. 7. Responses of sensors based on S0 and S1 at 230 °C to 200 ppm various gases.

to be continued, adsorption and desorption of HCHO molecules achieved dynamic equilibrium, it reached the best working temperature. Thus, the change in resistance would be decreased when working temperature reached a higher level. Namely, the sensitivity would be reduced. From another perspective, temperature of maximum response(TM) was gas-species dependent, as well as depended on the adsorbate(analyte) gas concentration. Furthermore, parameters SM (maximum response) and TM characterise the sensitivity distributions. The first of these parameters describes the strength of the analyte gas binding on the metal oxide surface and the second depicts the kinetic barrier that needs to be overcome to induce a surface combustion event [20]. Such considerations may also have an impact on the interpretation of the data compiled in Table 1.

Response and recovery times are important parameters for gas sensors. The sensing transients of S0 and S1 sensors to 10–1000 ppm formaldehyde at 230 °C are given in Fig. 5. It clearly showed that with the increase of formaldehyde concentration, the value of real-time response of both sensors increases obviously. From the curve, we could read out the response time (τres) and the recovery time (τrec) to 1000 ppm formaldehyde were 2 and 2 s, respectively, while response and recovery rate of S0 were relatively long. In addition, our τres and τrec of formaldehyde sensor is far more rapidly than most reported formaldehyde sensor, such as Li-doped NiO sensor [21] (response time10 s, recovery time 1–2 min), $Au@SnO_2$ sensor [22] (response time 80 s, recovery time 62 s). Response and Recovery time comparisons of various formaldehyde sensors are displayed in Table 2. An explanation of time constants maybe as followed: the response and recovery time constants to reactive analyte gases conform to a Meyer-Neldel compensation rule behavior. When the gas was injected into gas bottle, the sensor was exposed to a forced flow condition, and heterogeneous catalytic surface interactions were occurred. An influence of "micro-climate" affected on the MOS (metal oxide semiconductor) sensor response. Thus, gas response time of nano-scale metal oxide semiconductor gas sensor may also determined by the moving gas outlet technique [27,28].

The response of sensors using pristine SnO_2 and hierarchical Cu-doped SnO_2 samples versus the formaldehyde concentration ranging from 10 to 1000 ppm at 230 °C is shown in Fig. 6. From the curve, it is found that the responses of both sensors increased rapidly with increasing of the formaldehyde concentration and then gradually tended to saturation (S0 sensor) when the formaldehyde concentrations reached higher level. Obviously, the sensor based on S1 exhibited the higher response to formaldehyde at different concentrations compared with that based on S0 in the whole detecting range. Fig. 7 clearly shows that introduction of Cu in SnO_2 improved its sensing performance in terms of response, indicating that S1 possessing a better sensitive property to formaldehyde.

The gas sensing selectivity is another important parameter to evaluate the sensing ability of semiconductor materials. Fig. 7

Table 2
Response and recovery time comparisons of various gas sensors toward formaldehyde.

Material	Preparation method	Concentration (ppm)	Response time (s)	Recovery time (s)
SnO_2/In_2O_3 [17]	Electrospinning	10	20	40
Au@ SnO_2 [22]	Sol–gel	50	80	62
$LaFeO_3$ [23]	Hydrothermal	500	13	25
SnO_2 [24]	Acid-washing	100	13	35
ZnO [25]	Thermostat water bath	100	6.5	24
NiO [26]	Hydrothermal	100	50	150
Cu@SnO_2 in this paper	Solvothermal	1000	2	2

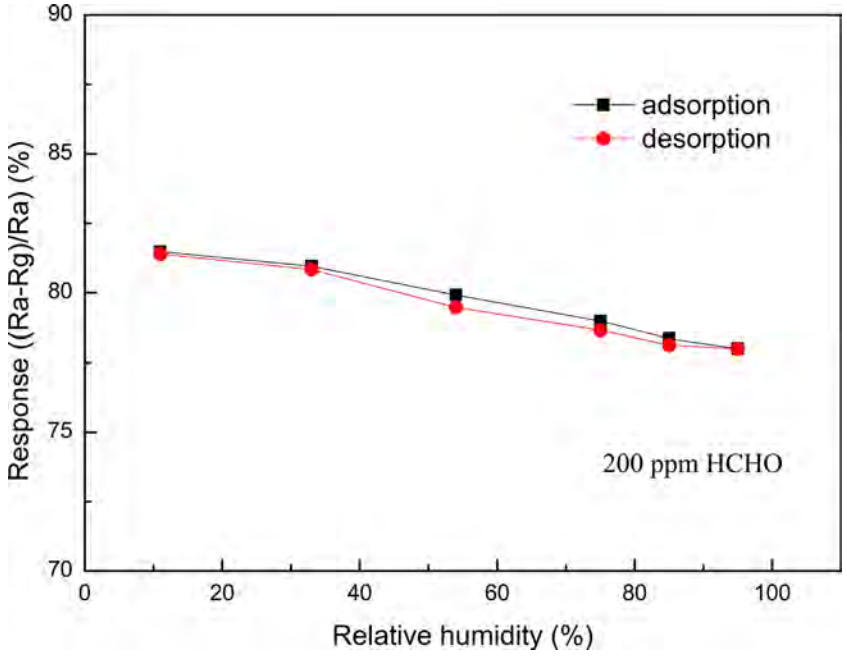

Fig. 8. Humidity hysteresis characteristics of the sensor based on Cu@SnO_2.

Table 3
Response and S_{HCHO}/S_{gas} comparisons of S0 and S1 gas sensors toward various gases.

Gas	$(R_a - R_g)/R_a$ (%) S0	S_{HCHO}/S_{gas} S0	$(R_a - R_g)/R_a$ (%) S1	S_{HCHO}/S_{gas} S1
SO_2	0.99	57.1	1.961	41.55
C_6H_6	0.99	57.1	5.66	14.4
C_2H_6O	2.534	22.3	5.66	14.4
NH_3	4.58	12.34	7.407	11
C_8H_{10}	6.455	8.76	9.091	8.96
C_3H_6O	9.42	6	13.04	6.25
C_2H_2	14.53	3.89	25.926	3.14
HCHO	56.52	1	81.48	1

shows the cross responses of sensors based on pristine SnO_2 and Cu-doped SnO_2 samples to a variety of gases with the concentration of 200 ppm, which were tested at their optimum operating temperatures of 230 °C. It can be observed that the response of S1 sensor to 200 ppm HCHO at 230 °C was 81.48, which was higher than the response to 200 ppm SO_2, C_6H_6, C_2H_6O, NH_3, C_8H_{10}, C_3H_6O, C_2H_2 (1.961–25.926). For the pristine SnO_2 sensor, the response to 200 ppm HCHO at 230 °C was 56.52, while those to most of other gases decreased (0.99–14.53). The selectivity to target gases was defined as the ratio of gas response to 200 ppm target gases and that to other gases $S_{HCHO}/Sgas$. $S_{HCHO}/Sgas$ values of interference gases were 3.89–57.1 for S0 sensor. And most of these values increased for S1 sensor (as shown in Table 3). Therefore, these results clearly demonstrated that sensor based on S1 was effective for selectivity toward formaldehyde. The better sensitivity for formaldehyde than other gases is considered to be caused by the different optimum working temperatures of the sensor to different gases. According to previous reports, the sensor showed selectivity at different operating temperature due to the distinction of the orbital energy of the gas molecule. Therefore, the doped mesoporous with hierarchical structure showed higher sensitivity to HCHO over other gases.

Fig. 8 shows humidity hysteresis characteristics of the sensor based on Cu@SnO_2, and the sensor was measured by DC voltage at increasing or decreasing RH(Relative Humidity) ranged from 11 to 95% (11, 33, 54, 75, 85, 95) at its optimum operating temperature 230 °C. The ratio of water vapor pressure and the saturated vapor pressure in the air was defined as the relative humidity. Our test procedure was as followed: The different RH conditions in this experiment were firstly prepared at the constant temperature 25 °C, and the RH range of 11–95% was obtained using saturated salt solutions as the humidity generation sources. After the RH conditions had been prepared, the sensor was placed into the 1 L bottle with different RH conditions to test target gas 200 ppm formaldehyde, and the DC power connected to Ni–Cr heating wire was turned on to provide the sensor's operating temperature 230 °C. All of the sensors' operating temperature were constant 230 °C provided by Ni–Cr heating wire(the length was about 5 mm), which only contributed to the sensitive material on the ceramic tube(the size was about 1 mm × 1 mm × 5 mm). 230 °C was mainly to provide operating temperature, which has no effect on the humidity in the whole test environment conditions. It can be observed that the Cu@SnO_2 sensor's response to 200 ppm formaldehyde decreases with the humidity increasing from 11 to 95% RH (adsorption process). When the humidity decreases from 95 to 11% RH (desorption progress), the sensor's response increases. The maximum

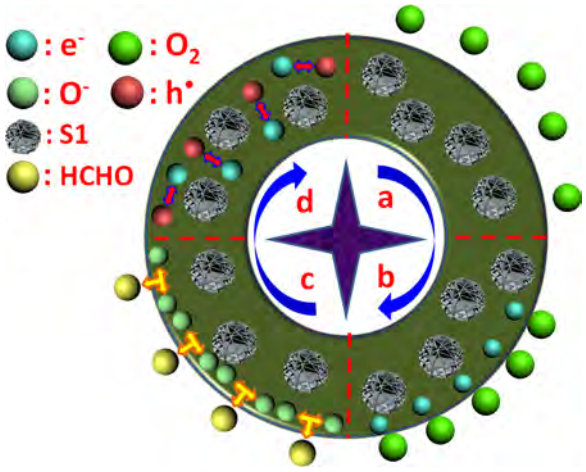

Fig. 9. Schematic illustration of gases conductive processes in the sensor system: (a) air atmosphere; (b) oxygen molecules trap electrons; (c) HCHO reacts with absorbed surface chemisorbed oxygen; (d) electrons reacts with holes.

hysteresis value is less than 1% RH, which shows good reliability of the sensing material, indicating that the hysteresis effect of the sensor was not too large to influence the application in real-world conditions. Thus, we found the fact that the response properties depended weakly on the amount of H_2O.

3.3. Gas sensing mechanism

In typically, the sensing mechanism could be explained through the change in resistance of the sensor caused by the adsorption and desorption process of gas molecules on the surface of the oxide [29–31]. In short, gas sensing process involves followed reactions: adsorption–oxidation–desorption. Adsorption mainly occurred on the surface of sensor. When S1 sensor is surrounded by air, chemisorbed oxygen species (O_2^-, O^-, O^{2-}) [32] were generated by adsorption of oxygen molecules, leading to a decrease in conductivity and increase in resistance of the sensor. The oxygen molecules capture electrons from Cu-doped SnO_2 and transforms into O^- (420–670 K), O^{2-} (above 670 K), and O_2^- (below 420 K) at the surface of sensing layer which would lead the holes to spread all over the surface of Cu-doped SnO_2 and the resistance increase [2]. When the sensor is exposed to reducing HCHO gas, HCHO molecules are adsorbed on the surface of Cu doped SnO_2, they are oxidized by chemisorbed oxygen species (O^-) and electrons are released back to the conduction band of the SnO_2, which will increase the carrier concentration and electron mobility, resulting in the reducing of sensor resistance (Schematic illustration is shown in Fig. 9). The reactions of HCHO with chemisorbed oxygen and lattice oxygen can be simply described as follows:

$$O_2(gas) + 2e^-(ads) \rightarrow 2O^-(ads) \quad (1)$$

$$HCHO(gas) + 2O^-(ads) \rightarrow CO_2 + H_2O + 2e^- \quad (2)$$

$$e^- + h^\bullet \leftrightarrow null \quad (3)$$

The quick response should be understood in the frame work of gas diffusion toward the SnO_2 surface and its reaction with surface oxygen species. At a stationary temperature, the surface reaction between HCHO and adsorbed oxygen will not vary significantly. Accordingly, gas diffusion could be regarded as the key factor. When the primary nanosheets are agglomerated to a significant extent, the target gas begins to interact with the nanosheets located at the outer part of SnO_2 sphere. In addition, the diffusion of the target gas toward the sensing surface of the interior particles requires a homologous time. On the one hand, the broad surfaces of nanosheets in hierarchical spherical structure become more reactive and likely to absorb oxygen and form ionized oxygen species, which can facilitate fast mass transfer of HCHO molecules to and from the interaction area as well as improve the rate for electrons. On another hand, the amount of oxygen that can be absorbed and ionized is increased induced by the increased specific area of the Cu-doped SnO_2. Thus, extraordinary architecture could be considered as a factor that promotes the device to absorb more HCHO molecules on the sensor. Moreover, the broad surface of nanosheets makes the absorption of oxygen and HCHO molecule easier, resulting in super-speed response and recovery.

Furthurmore, doping with other elements is one of the efficient ways to modify the physical and chemical properties of SnO_2 materials. The improvement of the response of Cu doped SnO_2 particles devices could attribute to the activation of Cu in enhancing the chemical activity of formaldehyde molecules. When Cu-doped SnO_2 spherical nanostructure was introduced to reductive HCHO atmosphere, substitution of Cu^+ for Sn^{4+} could enhance the active surface to more generation of surface oxygen vacancies according to the solid state chemistry theory, resulting in higher sensor responses. Furthermore, during adsorption and desorption on the surface of Cu, some of formaldehyde molecules are chemically more active. In this way, formaldehyde gas is easier to absorb on and react with the particles surface. Copper replacement of tin in SnO_2 lattice may form certain amounts of catalytically active centre [33], which work effectively as centres of the oxygen chemisorption and reducing gases oxidation, providing electronic exchange between absorbed species and the SnO_2 conduction band. Thus, above mechanism would lead to optimization of adsorption/desorption dynamic equilibrium at the SnO_2 surface, controlling gas sensing effects, and contributing to changes of gas sensing properties. This will explained rapid response-recovery speed and increase in the response of SnO_2 sensors after Cu doping. In the end, the reason for the pronounced gas response to formaldehyde maybe as followed: comparing the gases investigated, the remarkable difference of formaldehyde with regard to the other ones is that formaldehyde contains a carbonyl (C═O) bond. The higher reactivity of C═O double bonds as compared to the C—H and N—H bonds in the other analytes was very likely the main factor to cause the pronounced gas response to formaldehyde. Certainly, our group is still in the further research of the mechanism.

4. Conclusions

In summary, pure SnO_2 and Cu doped SnO_2 were synthesized through a solvothermal method and their HCHO sensing properties were investigated. The results showed that Cu-doping can improve their HCHO sensing performance greatly compared to pure SnO_2. SnO_2 sensor with Cu doping exhibited the highest response and best selectivity among all the samples. The improvement of sensing properties was attributed to the increase of oxygen vacancy induced by the Cu doped and extensive surface area of hierarchical SnO_2 structure which have been well activated and utilized for gas sensing.

Acknowledgements

The authors are grateful to National Natural Science Foundation of China (Grant 61274068, 11574110), the National High Technology Research and Development Program of China (Grant No. 2013AA030902), Opened Fund of the State Key Laboratory on Integrated Optoelectronics (No. IOSKL2013KF10), and Project of Science and Technology Plan of Changchun City (Grant No. 14KG020).

References

[1] Lee Jong-Heun, Gas sensors using hierarchical and hollow oxide nanostructures: overview, Sens. Actuators B 140 (2009) 319–336.
[2] Fengdong Qu, Juan Liu, Ying Wang, Shanpeng Wen, Yu Chen, Xu Li, Shengping Ruan, Hierarchical Fe_3O_4@Co_3O_4 core–shell microspheres: preparation and acetone sensing properties, Sens. Actuators B 199 (2014) 346–353.
[3] Murukanahally Kempaiah Devaraju, Itaru Honma, Hydrothermal and solvothermal process towards development of $LiMPO_4$ (M = Fe, Mn) nanomaterials for lithium-ion batteries, Adv. Energy Mater. 2 (2012) 284–297.
[4] Tetsuya Kida, Aya Nishiyama, Zhongqiu Hua, Koichi Suematsu, Masayoshi Yuasa, Kengo Shimanoe, WO_3 nanolamella gas sensor: porosity control using SnO_2 nanoparticles for enhanced NO_2 sensing, Langmuir 30 (2014) 2571–2579.
[5] G.R. Mohimann, Formaldehyde detection in air by laser-induced fluorescence, Appl. Spectrosc. 39 (1985) 98–101.
[6] Emma Tait, Stephen P. Stanforth, Stephen Reed, John D. Perry, John R. Dean, Analysis of pathogenic bacteria using exogenous volatile organic compound metabolites and optical sensor detection, RSC Adv. 5 (2015) 15494.
[7] Jeffrey M. Lorrain, Christopher R. Fortune, Barry Dellinger, Sampling and ion chromatographic determination of formaldehyde and acetaldehyde, Anal. Chem. 3 (1981) 1303.
[8] Siddharth Maheshwari, Hsueh-Chia Chang, Assembly of multi-stranded nanofiber threads through AC electrospinning, Adv. Mater. 21 (2009) 349–354.
[9] Xiaogang Peng, Band gap and composition engineering on a nanocrystal (BCEN) in solution, Acc. Chem. Res. 43 (2010) 1387–1395.
[10] Michelled D. Regulacio, MingYong Han, Composition-tunable alloyed semiconductor nanocrystals, Acc. Chem. Res. 43 (2010) 621–630.
[11] D.D.D. Ma, C.S. Lee, F.C.K. Au, S.Y. Tong, S.T. Lee, Small-diameter silicon nanowire surfaces, Science 299 (2003) 1874–1877.
[12] Caihui Feng, Wei Li, Chao Li, Linghui Zhu, Haifeng Zhang, Ying Zhang, Shengping Ruan, Weiyou Chen, Lianxiang Yu, Highly efficient rapid ethanol sensing based on $In_{2-x}Ni_xO_3$ nanofibers, Sens. Actuators B 166–167 (2012) 83–88.
[13] Linghui Zhu, Dezhong Zhang, Ying Wang, Caihui Feng, Jingran Zhou, Caixia Liu, Shengping Ruan, Xylene gas sensor based on Ni doped TiO_2 bowllike submicron particles with enhanced sensing performance, RSC Adv. 5 (2015) 28105.
[14] Xiao Chi, Changbai Liu, Li Liu, Shouchun Li, Haiying Li, Xiaobo Zhang, Xiaoqing Bo, Hao Shan, Enhanced formaldehyde-sensing properties of mixed Fe_2O_3–In_2O_3 nanotubes, Mater. Sci. Semicond. Process. 18 (2014) 160–164.
[15] Hyung Ju Park, Nak-Jin Choi, Hyuntae Kang, Moon Youn Jung, Jeong Won Park, Kang Hyun Park, Dae-Sik Lee, A ppb-level formaldehyde gas sensor based on CuO nanocubes prepared using a polyol process, Sens. Actuators B 203 (2014) 282–288.
[16] Shahid Hussain, Tianmo Liu, M. Kashif, Shixiu Cao, Wen Zeng, Sibo Xu, Khalid Naseer, Uha Hashim, A simple preparation of ZnO nanocones and exposure to formaldehyde, Mater. Lett. 128 (2014) 35–38.
[17] Haiying Du, Jing Wang, Yanhui Sun, Penjun Yao, Xiaogan Li, Naisen Yu, Investigation of gas sensing properties of SnO_2/In_2O_3 composite hetero-nanofibers treated by oxygen plasma, Sens. Actuators B 206 (2015) 753–763.
[18] N.G. Pramod, S.N. Pandey, Effect of Li doping on the structural, optical and formaldehyde sensing properties of In_2O_3 thin films, Ceram. Int. 41 (2015) 527–532.
[19] Keng Xu, Dawen Zeng, Jinjin Wu, Qiangqiang Mao, Shouqin Tian, Shunping Zhang, Changsheng Xie, Correlation between microstructure and gas sensing properties of hierarchical porous tin oxide topologically synthesized on coplanar sensors' surface, Sens. Actuators B 205 (2014) 416–425.
[20] S. Ahlers, G. Müller, T. Doll, A rate equation approach to the gas sensitivity of thin film metal oxide materials, Sens. Actuators B: Chem. 107 (2005) 587–599.
[21] Jae Young Kim, Nak-Jin Choi, Hyung Ju Park, Jinmo Kim, Dae-Sik Lee, Hyunjoon Song, A hollow assembly and its three-dimensional network formation of single-crystalline Co_3O_4 nanoparticles for ultrasensitive formaldehyde gas sensors, J. Phys. Chem. C 118 (2014) 25994–26002.
[22] Feng-Chao Chung, Ren-Jang Wu, Fu-Chou Cheng, Fabrication of a Au@SnO_2 core-shell structure for gaseous formaldehyde sensing at room temperature, Sens. Actuators B 190 (2014) 1–7.
[23] Jian Qin, Zhenduo Cui, Xianjin Yang, Shengli Zhu, Zhaoyang Li, Yanqin Liang, Synthesis of three-dimensionally ordered macroporous $LaFeO_3$ with enhanced methanol gas sensing properties, Sens. Actuators B 209 (2015) 706–713.
[24] Jiarui Huang, Liyou Wang, Cuiping Gu, Zhijun Wang, Yufeng Sun, Jae-Jin Shim, Preparation of porous SnO_2 microcubes and their enhanced gas-sensing property, Sens. Actuators B 207 (2015) 782–790.
[25] Jianwei Zhao, Changsheng Xie, Li Yang, Shunping Zhang, Guozhu Zhang, Ziming Cai, Enhanced gas sensing performance of Li-doped ZnO nanoparticle film by the synergistic effect of oxygen interstitials and oxygen vacancies, Appl. Surf. Sci. 330 (2015) 126–133.
[26] Xiaohong Sun, Xudong Hu, Yongchao Wang, Rui Xiong, Xin Li, Jing Liu, Huiming Ji, Xiaolei Li, Shu Cai, Chunming Zheng, Enhanced gas-sensing performance of Fe-doped ordered mesoporous NiO with long-range periodicity, J. Phys. Chem. C 119 (2015) 3228–3237.
[27] A. Helwig, G. Müller, G. Sberveglieri, G. Faglia, Gas response times of nano-scale SnO_2 gas sensors as determined by the moving gas outlet technique, Sens. Actuators B: Chem. 126 (2007) 174–180.
[28] A. Helwig, G. Müller, G. Sberveglieri, G. Faglia, Catalytic enhancement of SnO_2 gas sensors as seen by the moving gas outlet method, Sens. Actuators B: Chem. 130 (2008) 193–199.
[29] Jinsoo Park, Xiaoping Shen, Guoxiu Wang, Solvothermal synthesis and gas-sensing performance of Co_3O_4 hollow nanospheres, Sens. Actuators B 136 (2009) 494–498.
[30] Jiaqiang Xu, Xiaohua Wang, Guoqing Wang, Jianjun Han, Yu'an Sun, Solvothermal synthesis of In_2O_3 nanocrystal and its ethanol sensing mechanism, Electrochem. Solid State Lett. 9 (11) (2006) H103–H107.
[31] Binni Varghese, Teo Choon Hoong, Zhu Yanwu, Mogalahalli V. Reddy, Bobba V.R. Chowdari, Andrew Thye Shen Wee, Tan B.C. Vincent, Chwee Teck Lim, Chorng-Haur Sow, Co_3O_4 nanostructures with different morphologies and their field—emission properties, Adv. Funct. Mater. 17 (2007) 1932–1939.
[32] Xiujuan Xu, Huitao Fan, Yantong Liu, Lijie Wang, Tong Zhang, Au-loaded In_2O_3 nanofibers-based ethanol micro gas sensor with low power consumption, Sens. Actuators B 160 (2011) 713–719.
[33] G. Korotcenkov, I. Boris, V. Brinzari, S.H. Han, B.K. Cho, The role of doping effect on the response of SnO_2-based thin film gas sensors: analysis based on the results obtained for Co-doped SnO_2 films deposited by spray pyrolysis, Sens. Actuators B 182 (2013) 112–124.

Biographies

Ying Wang received the bachelor degree from the College of Electronic Science and Engineering, Jilin University, China in 2013. Now, she is a graduate student and engaged in synthesis and analysis of functional materials and gas sensors.

Dingsheng Jiang received the bachelor degree from the College of Electronic Science and Engineering, Jilin University, China in 2014. Now, he is a graduate student and interested in functional materials and gas sensors.

Wei Wei received the bachelor degree from the College of Electronic Science and Engineering, Jilin University, China in 2014. Now, he is a graduate student and working for a master's degree and interested in functional materials and gas sensors.

Linghui Zhu received the bachelor degree from the College of Electronic Science and Engineering, Jilin University, China in 2011. She is currently studying for a doctor's degree and devoting herself to the research of functional nanomaterials, chemical sensors and photodetector.

Jingran Zhou received his PhD degree in the College of Electronic Science and Engineering, Jilin University, China in 2005. Now he is an assistant professor in the College of Electronics Science and Engineering, Jilin University, and interested in the field of characterizing and testing of the materials.

Dongming Sun works in the State Key Laboratory on Integrated Optoelectronics, Jilin University. He is mainly devoted to the research of chemical sensor.

Shengping Ruan received the PhD degree of electronic science and engineering from Jilin University in 2001. Now, he is a full professor in the College of Electronics Science and Engineering, Jilin University, and mainly devoted to the research of electronic functional materials and devices.